

Rashba spin precession in quantum Hall edge channels

Marco G. Pala

*Dipartimento di Ingegneria dell'Informazione, Università degli Studi di Pisa, via Caruso, I-56122 Pisa, Italy and
Institut für Theoretische Festkörperphysik, Universität Karlsruhe, D-76128 Karlsruhe, Germany*

Michele Governale

NEST-INFM & Scuola Normale Superiore, piazza dei Cavalieri 7, I-56126 Pisa, Italy

Ulrich Zülicke

*Institute of Fundamental Sciences, Massey University,
Private Bag 11 222, Palmerston North, New Zealand*

Giuseppe Iannaccone

*Dipartimento di Ingegneria dell'Informazione, Università degli Studi di Pisa, via Caruso, I-56122 Pisa, Italy and
IEIIT-Consiglio Nazionale delle Ricerche, via Caruso, I-56122 Pisa, Italy*

(Dated: November 6, 2018)

Quasi-one dimensional edge channels are formed at the boundary of a two-dimensional electron system subject to a strong perpendicular magnetic field. We consider the effect of Rashba spin-orbit coupling, induced by structural inversion asymmetry, on their electronic and transport properties. Both our analytical and numerical results show that spin-split quantum-Hall edge channels exhibit properties analogous to that of Rashba-split quantum wires. Suppressed backscattering and a long spin life time render these edge channels an ideal system for observing voltage-controlled spin precession. Based on the latter, we propose a magnet-less spin-dependent electron interferometer.

PACS numbers: 85.75.-d, 73.43.-f, 73.63.-b

I. INTRODUCTION

Spin-dependent transport in semiconductors has attracted a lot of interest recently, due to intriguing new physics phenomena that are observed experimentally or predicted theoretically.^{1,2} Some of these may form the basis of future device applications within the spintronics paradigm, where information is coded and transferred using the spin degree of freedom instead of charge.³ External magnetic fields and magnetic contacts provide a possible means to control the spin of charge carriers.⁴ Spin control via spin-orbit (SO) coupling, which is interesting from a fundamental-physics viewpoint⁵ and possibly useful for device application,⁶ has gained prominence recently as an intriguing alternative to the use of magnetic systems. In particular, the Rashba-type SO coupling^{7,8,9} which arises from structural inversion asymmetry in semiconductor heterostructures is of particular interest to spintronics research, as its strength can be tuned by external gate voltages.^{10,11,12,13}

At the same time as enabling novel spin-dependent transport effects, SO coupling is also responsible for spin-relaxation phenomena that limit the operation of spintronics devices. For mesoscopic electron transport in semiconductors, the Dyakonov-Perel mechanism¹⁴ is the dominant source of spin relaxation. It is due to elastic scattering which randomizes the orientation of momentum and, via SO coupling, the spin orientation. This mechanism limits experimental observation of coherent spin-dependent transport phenomena, such as spin precession in magnetic fields or due to the Rashba effect.⁵

Here we consider a system well-suited to the study of spin-dependent transport effects, due to its relatively weak spin relaxation: a two-dimensional (2D) electron system in the integer quantum Hall (QH) regime.¹⁵ The latter is realized when a perpendicular magnetic field B is applied such that the filling factor $\nu = 2\pi l_B^2 n_{2D}$ assumes integer values (here $l_B = \sqrt{\hbar/|eB|}$ is the magnetic length, and n_{2D} the electronic sheet density). Then a bulk incompressibility occurs in the 2D electron system and, for a sufficiently steep confining potential at the sample boundaries, transport is possible only via chiral quasi-one dimensional edge channels.^{16,17,18} The spatial separation of right-moving and left-moving edge channels by the incompressible bulk prevents backscattering. Furthermore, long equilibration lengths between opposite-spin QH edge states (of the order of 100 μm) have been observed in GaAs-based samples.^{19,20} Spin flips induced by impurity scattering in the presence of SO coupling were found^{19,21} to be the dominant mechanism for spin relaxation in the QH regime. Hence, the typically stronger SO coupling in InAs-based 2D heterostructures should reduce spin life times for QH edge channels realized in such samples. Indeed, for identical quantum-well parameters (such as width, sheet and donor densities) and edge-channel profiles, the ratio of spin-relaxation lengths l_{sf} in the InAs and GaAs materials systems can be approximated, in the high-field limit, by^{21,22}

$$\frac{l_{\text{sf}}^{\text{InAs}}}{l_{\text{sf}}^{\text{GaAs}}} \approx \left| \frac{g_{\text{InAs}}}{g_{\text{GaAs}}} \right| \left(\frac{L_{\text{so}}^{\text{InAs}}}{L_{\text{so}}^{\text{GaAs}}} \right)^2 \sim 0.1 \text{ typically} \quad . \quad (1)$$

We have denoted the gyromagnetic ratio by g , and L_{so} is the spin-precession length due to the strongest spin-orbit coupling present in the respective materials (Rashba-type for InAs, Dresselhaus-type²³ for GaAs²¹). From our rough estimate, we would expect the spin-flip length l_{sf} in InAs-based QH edge channels to exceed tens of microns, which is much larger than the spin-precession length L_{so} that determines, e.g., the gate length in a spin-controlled field-effect transistor.^{5,24} This motivates our study of spin-dependent transport in Rashba-split QH edge channels.

Previous studies of magnetotransport in the presence of Rashba spin splitting have focused on beating patterns in the Shubnikov-de Haas oscillations,^{25,26} the Hall resistance,²⁶ and quasi-one dimensional point-contact conductances.²⁷ The interplay between spin-orbit coupling and cyclotron motion was discussed recently²⁸ in the weak-magnetic-field regime with particular emphasis on using magnetic focusing to separate electrons according to their spin state.²⁹

In this paper we present a theory for QH edge states with Rashba SO coupling in the strong field regime where the Rashba spin splitting is much smaller than the cyclotron energy. We give an analytical approximation for the Landau-level dispersions, both for the case when the Zeeman term is negligible and when the Zeeman splitting is comparable to the Rashba one. Our analytical results show that QH edge states in the presence of Rashba SO coupling behave, as far as spin precession is concerned, in a very similar way to Rashba-split quantum wires.^{27,30,31} Furthermore, we study spin transport in edge channels by means of the numerical recursive-Green's-function technique without making any of the approximations that were necessary to obtain analytical results. The numerical transport calculations allow us to test the validity of our analytical Landau-level description when used to describe linear transport.

The paper is organized as follows. We introduce the theoretical description in Sec. II and give analytical results on Landau-level dispersions. In Sec. III we present numerical results on spin-dependent transport and test the validity of approximations made in Sec. II. Sec. IV is devoted to a discussion of an interferometer setup, suitable for observing interference effects due to spin precession. Conclusions are given in Sec. V.

II. THEORETICAL DESCRIPTION AND ANALYTICAL RESULTS

In this section, we introduce the model Hamiltonian for our system of interest. Analytical results are presented, within certain approximations, for edge-channel energy dispersions and wave functions with Rashba SO coupling.

We study a two-dimensional electron system in the xy plane, subject to a homogeneous perpendicular magnetic field $\mathbf{B} = B\hat{\mathbf{z}}$, and confined laterally (in y direction) by the boundary potential $V(y)$. Translational invariance

in x direction suggests the use of the Landau gauge with vector potential $\mathbf{A} = -By\hat{\mathbf{x}}$. Furthermore, we assume that the electrons are subject to a SO coupling of the Rashba type,⁷ and neglect the SO coupling arising from bulk inversion asymmetry.^{23,32} This is reasonable as a first approximation to describe realistic InAs quantum-well systems.^{33,34} The Hamiltonian of the system is then given by $H = H_0 + H_{\text{R}} + H_Z$, with

$$H_0 = \frac{1}{2m^*} [(p_x + eBy)^2 + p_y^2] + V(y), \quad (2a)$$

$$H_{\text{R}} = \frac{\alpha_{\text{R}}}{\hbar} [\sigma_x p_y - \sigma_y (p_x + eBy)], \quad (2b)$$

$$H_Z = \frac{g}{2} \mu_B B \sigma_z = \frac{\nu_Z}{2} \sigma_z, \quad (2c)$$

where m^* is the effective mass, e (< 0) the electron charge, \vec{p} the canonical momentum, α_{R} measures the strength of Rashba SO coupling, and $\mu_B = |e|\hbar/2m_e$ denotes the Bohr magneton. In the following, it will be useful to express the SO coupling strength in terms of a length scale, $l_{\text{R}} = \hbar^2/(m^* \alpha_{\text{R}})$, which is related to the spin-precession length^{5,24} L_{so} mentioned in the previous section via $l_{\text{R}} = L_{\text{so}}/\pi$. Our study focuses on the high-field regime where $l_B < l_{\text{R}}$.

A. Results in the absence of Zeeman splitting

We start by discussing the case of vanishing Zeeman splitting. The validity of this approximation is discussed in the next subsection, where the effect of the Zeeman splitting on the edge states is studied at the level of perturbation theory. We furthermore neglect the term $(\alpha_{\text{R}}/\hbar)\sigma_x p_y$ from the Rashba Hamiltonian. This approximation, which we call *longitudinal SO approximation*,³⁰ turns out to be valid, in the high-field regime, when the transverse width of the QH states is smaller than the SO length l_{R} and the transport becomes quasi-one dimensional [note that the transverse Rashba term $(\alpha_{\text{R}}/\hbar)\sigma_x p_y$ becomes important, e.g., at Landau-level crossings^{28,35}]. The Hamiltonian can now be written as

$$\tilde{H} = \frac{p_y^2}{2m^*} + \frac{m^* \omega_c^2}{2} \left(\hat{Y} + y - \frac{l_B^2}{l_{\text{R}}} \sigma_y \right)^2 + V(y), \quad (3)$$

where $\hat{Y} = (p_x/\hbar)l_B^2 \text{sgn}(eB)$ is the operator of guiding-center coordinate for cyclotron motion, and $\omega_c = |eB|/m^*$ the cyclotron frequency. In writing Eq. (3), we have neglected a constant energy shift of order $\hbar^2/(m^* l_{\text{R}}^2)$, which is small compared to the cyclotron gap. For the eigenfunctions of Hamiltonian (3), we make the *Ansatz*

$$\psi_{n,Y,\sigma}(x, y) = e^{iYx/l_B^2} \phi_{n,Y,\sigma}(y) |\sigma_y\rangle, \quad (4)$$

where $|\sigma_y\rangle$ is the eigenspinor of the Pauli matrix σ_y with eigenvalue $\sigma = \pm 1$. Substituting the *Ansatz* Eq. (4) in the Schrödinger equation, we find the eigenenergies

$$E_n(Y) = E_n^{(0)} \left(Y - \sigma \frac{l_B^2}{l_{\text{R}}} \right) \quad . \quad (5)$$

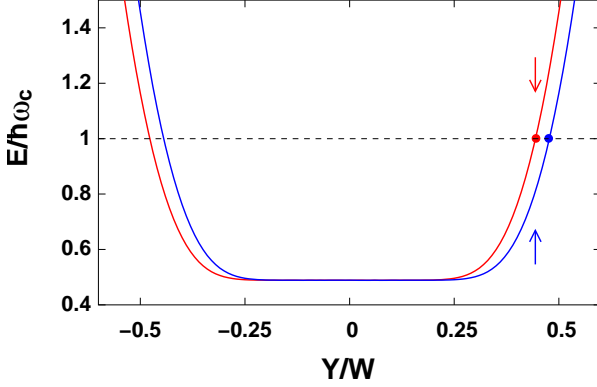


FIG. 1: (Color online) Dispersion of the lowest Landau level, calculated within the longitudinal SO approximation, for a hard-wall confining potential of width W . The labels \uparrow, \downarrow refer to eigenvalues of σ_y . The parameters used are: $L_{\text{so}}/l_B = 21.3$, and $W/l_B = 8.9$.

Here $E_n^{(0)}(Y)$ are the Landau-level dispersions in the absence of Rashba SO coupling. The transverse eigenfunctions are given by

$$\phi_{n,Y,\sigma}(y) = \phi_{n,Y-\sigma l_R^2}^{(0)}(y), \quad (6)$$

where $\phi_{n,Y}^{(0)}(y)$ are the corresponding transverse eigenfunctions without Rashba SO coupling.

At this point a few comments are necessary. Within the longitudinal SO approximation, the effect of the Rashba SO coupling is to shift Landau levels with different spin quantum number σ in the guiding-center quantum number Y . An example of a Landau-level dispersion is shown in Fig. 1. In this limit, a global spin-quantization axis exists, which is perpendicular to the system boundary and in the plane of the 2D electron system. This is analogous to what happens in quantum wires in the weak-SO-coupling regime.³¹ As these properties are those on which the design of a spin-controlled field-effect transistor (SpinFET) relies,⁵ we can conclude that a prototype of the SpinFET could be implemented using QH edge channels. Such a system would realize the ideal situation of a highly one dimensional transport regime²⁷ and slow spin relaxation from elastic scattering.

The quantum numbers $Y_{n,\sigma}$ of the guiding-center coordinate in y direction for edge states at a fixed energy E are given by

$$Y_{n,\sigma} = Y_n^{(0)} + \sigma l_B^2/l_R, \quad (7)$$

where $Y_n^{(0)}$ satisfies $E_n^{(0)}(Y_n^{(0)}) = E$. The guiding-center separation for states at fixed energy turns out to not depend on this energy or the Landau-level index n ; we find

$$\Delta Y = 2l_B^2/l_R. \quad (8)$$

It is important to notice that the density profile in confinement direction for wave functions (6) corresponding

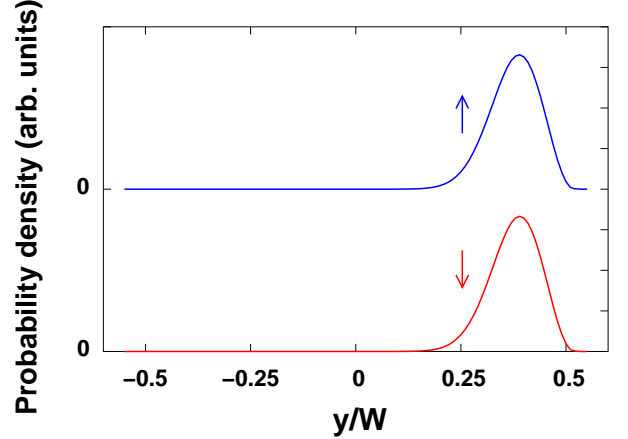


FIG. 2: (Color online) Transverse probability-density profile for spin up (top) and spin down (bottom) right-moving edge states at a fixed energy $E = \hbar\omega_c$. The transverse probability densities, shown here, correspond to the states marked by a dot in Fig. 1. The spin labels \uparrow, \downarrow refer to eigenvalues of σ_y . Parameters are the same as in Fig. 1.

to spin-split edge states [i.e., with guiding centers $Y_{n,\sigma}$ given in Eq. (7)] is the same, and is simply $|\phi_{Y_n^{(0)}}^{(0)}(y)|^2$. This last remark means that although edge states with different spin are shifted in their guiding-center *quantum number*, they are *not separated spatially* (see Fig. 2).

For small l_B/l_R , we can expand the Landau level dispersion Eq. (5) to first order around Y , obtaining

$$E_n(Y) \approx E_n^{(0)}(Y) - \sigma \frac{l_B^2}{l_R} \frac{\partial E_n^{(0)}(Y)}{\partial Y}. \quad (9)$$

From Eq. (5), and even more from Eq. (9), it is apparent that bulk Landau levels, which are non dispersive, are not affected to first order in l_B/l_R by Rashba SO coupling. This is in agreement with the exact solution for bulk Landau levels given in Ref. 7, where the first non vanishing correction to eigenenergies is quadratic in l_B/l_R .

B. Effect of finite Zeeman splitting

In the previous subsection, we neglected the Zeeman effect. We now discuss how a finite but small Zeeman splitting affects spin precession in QH edge channels.

The value of spin splitting due to the Zeeman effect can be expressed as

$$\nu_Z = \frac{gm^*}{2m_e} \hbar\omega_c, \quad (10)$$

whereas the Rashba spin splitting for an edge state with guiding center Y is given by

$$\nu_R(Y) = 2 \frac{l_B^2}{l_R} \frac{\partial E_n^{(0)}(Y)}{\partial Y} = \frac{2\hbar}{l_R} v_n^{(0)}(Y). \quad (11)$$

Here $v_n^{(0)} = (l_B^2/\hbar) \partial E_n^{(0)}/\partial Y$ is the group velocity of edge states on the n^{th} unperturbed Landau level. For a boundary confining potential that is rising sharply on the scale of the magnetic length, it can be estimated as $v_n^{(0)} \approx \omega_c l_B$, yielding

$$\left| \frac{\nu_Z}{\nu_R} \right| = \frac{g}{4} \frac{m^*}{m_e} \frac{l_R}{l_B} = \frac{0.7 g \sqrt{B[T]}}{\alpha_R [10^{-12} \text{ eV m}]} . \quad (12)$$

For typical values in InAs heterostructures,³⁶ the Zeeman splitting becomes comparable to the Rashba spin splitting at a magnetic field of ~ 8 Tesla. Note, however, that edge velocities at soft sample-boundary potentials can be an order of magnitude smaller than the estimate used above.

In the situation when the Zeeman and the Rashba splitting are comparable and both are much smaller than $\hbar\omega_c$, we can perform a perturbative calculation, finding for the Landau-level dispersions²¹:

$$E_n^{\pm}(Y) = E_n^{(0)}(Y) \mp \frac{1}{2} \sqrt{\nu_R(Y)^2 + \nu_Z^2} . \quad (13)$$

After performing a perturbative calculation on a spin-degenerate subspace, we find that the orbital part of the eigenfunctions is unchanged, while the eigenspinors read

$$\begin{aligned} \chi^+(Y) &= \begin{pmatrix} \sin[\theta(Y)/2] \\ i \cos[\theta(Y)/2] \end{pmatrix}, \\ \chi^-(Y) &= \begin{pmatrix} \cos[\theta(Y)/2] \\ -i \sin[\theta(Y)/2] \end{pmatrix}, \end{aligned} \quad (14)$$

with $\tan[\theta(Y)] = \nu_Z/\nu_R(Y)$. If we set $\nu_Z = 0$ in Eqs. (13,14) we find the Landau level dispersions given in Eq. (9), and the eigenspinors become $|\sigma_y\rangle$. In the presence of the Zeeman term, the eigenspinor quantization axis depends on Y . In particular, it does not lie anymore in the xy plane, but it sticks out of it; the in-plane component remaining still perpendicular to the boundary (i.e., parallel to y). The new eigenspinors Eq. (14) are parallel to the effective magnetic field $\mathbf{B}_{\text{eff}}(Y) = \mathbf{B} + \mathbf{B}_R(Y)$, where \mathbf{B}_R is the effective Rashba field (the Rashba term can be viewed as a Zeeman term with a momentum dependent magnetic field), which in our case is $\mathbf{B}_R(Y) = -(\nu(Y)/g\mu_B)\hat{y}$.

III. SPIN-DEPENDENT TRANSPORT: NUMERICAL RESULTS

Our results obtained in the previous section showed that, within the longitudinal SO approximation and for vanishing Zeeman splitting, QH edge-channel eigenspinors are polarized in the direction perpendicular to the sample boundary and in the plane of the QH system. In that situation, spin precession will occur for electrons injected with spins parallel to the edge, e.g., by a magnetic contact. This is entirely analogous to the

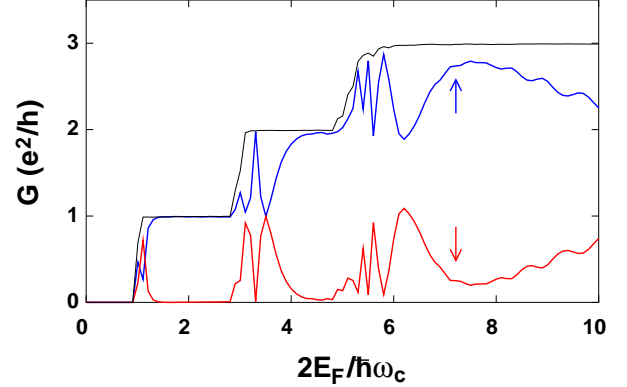


FIG. 3: (Color online) Spin-polarized conductances as a function of the inverse magnetic field $1/\hbar\omega_c$ for fixed Fermi energy E_F . The blue line represents $G_{\uparrow\uparrow}$, the red line $G_{\downarrow\uparrow}$, and the black line $G_{\uparrow\uparrow} + G_{\downarrow\uparrow}$. The Zeeman coupling is set to zero. The other parameters are: $L/\lambda_F = 40$, $W/\lambda_F = 2$, $L_{\text{SO}} = L/5$, λ_F denotes the Fermi wave length.

operational principle of a SpinFET.⁵ To test the validity of the underlying approximations made to obtain our analytical results, we have studied spin-dependent edge-channel transport, in the presence of Rashba SO coupling and Zeeman splitting, numerically without making any of the approximations of the previous section.

We compute total and spin-polarized linear conductances of a finite-size QH system within the framework of the Landauer-Büttiker theory,³⁷ assuming the zero-temperature limit. A tight-binding model is adopted to describe the Hamiltonian of the system,³⁰ and we use a recursive method to obtain the total Green's function of the system.^{38,39,40} Projecting the Green's function on asymptotic waves in the leads and on spin-up and spin-down eigenspinors, transmission and reflection coefficients are immediately obtained.^{39,41} The conductance is expressed by the Landauer-Büttiker formula

$$G = \frac{e^2}{h} \sum_{nn'} \sum_{\sigma\sigma'} |t_{n'n}^{\sigma'\sigma}|^2 , \quad (15)$$

where the sum runs over all incoming and outgoing channels, and $t_{n'n}^{\sigma'\sigma}$ is the transmission amplitude from mode n with spin σ to mode n' having spin σ' . We assume that the system is attached to external leads with the same homogeneous magnetic field as present in the sample, but without SO coupling. In the external leads, we choose z as spin quantization axis and, in this Section, “up” and “down” always refers to eigenspinors of σ_z . Together with the total conductance, we calculate $G_{\sigma\uparrow}$, i.e., the conductance obtained by injecting a spin-up current and detecting a spin- σ current at the output contact.

In Fig. 3, we show examples of spin-polarized conductances, plotted as a function of the inverse magnetic field, for a fixed Fermi energy and zero Zeeman splitting. The total conductance $G_{\uparrow\uparrow} + G_{\downarrow\uparrow}$ (for injection of up-spins) presents the usual step-like behavior, whereas the spin-

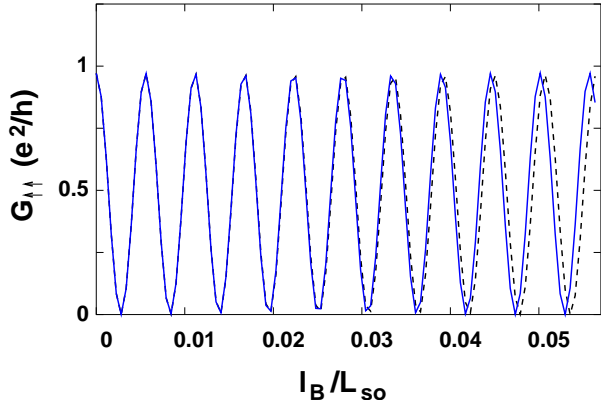


FIG. 4: (Color online) Conductance $G_{\uparrow\uparrow}$ of the spin-up edge channel at filling factor one, computed both with transverse Rashba term (solid line) and without it (dashed line) and plotted here as a function of the Rashba SO coupling strength. The Zeeman coupling is set to zero. The other parameters are: $E/\hbar\omega_c = 1$, $L/\lambda_F = 40$, $W/\lambda_F = 2$.

polarized ones have an irregular shape that depends on the spin precession length.

In Fig. 4, we test the validity of the longitudinal SO approximation. We plot $G_{\uparrow\uparrow}$ as a function of the SO coupling strength, computed with and without the longitudinal SO approximation. The two curves coincide perfectly for small Rashba coupling and start differing slightly when the SO coupling becomes large.

Now, we turn our attention to the interplay between the Rashba SO coupling and the Zeeman splitting.⁴² In Fig. 5, we show spin-polarized conductances as a function of both g -factor and SO coupling strength (expressed in terms of the spin precession length). The effect of the Zeeman splitting is to induce a finite z -component in the effective magnetic field \mathbf{B}_{eff} around which the spin precesses. When $g = 0$, the effective field \mathbf{B}_{eff} lies in the plane of the 2D electron system and, hence, it is orthogonal to the z -axis and the current modulation is largest. In the opposite limit, the Zeeman coupling tends to align the eigenspinors along the z -direction, and spin-precession gets weaker. We conclude that the presence of the Zeeman splitting has a negative effect on the spin precession, but it does not disrupt it as long as $|\nu_R/\nu_Z| > 1$.

IV. SPIN-DEPENDENT EDGE-CHANNEL INTERFEROMETERS

In this Section, we investigate the possibility to observe spin-dependent interference effects between edge channels. This study is motivated by a recent experimental realization of an electronic analog of the optical Mach-Zehnder interferometer.⁴³ Spin-dependent electron interferometry based on Rashba spin splitting has recently been discussed, in zero magnetic field, in Refs. 44,45.

Edge channels are a very useful tool to construct electronic analogs of optical experiments, due to their chiral nature. Key elements of many optical interferometers are beam splitters and wave guides. Both these building blocks have been realized for electron waves in suitably designed nanostructures.⁴³ The schematic setup of a possible spin-dependent edge-channel interferometer is sketched in Fig. 6. A right-moving edge channel is split by QPC1 into two different outgoing channels. These two states travel along a straight segment of length L , perform an abrupt bend and, after another segment of length L , interfere at QPC2.

We consider the case of one propagating edge channel (filling factor one) and the presence of both Rashba and Zeeman splittings. The question we want to answer is whether a current modulation can be induced by varying only the strength of Rashba SO coupling. Let us discuss, for the sake of simplicity, the situation depicted in Fig. 6. If the incident spinor Ψ_{in} is split evenly at QPC1, the outgoing spinor at QPC2 reads

$$\Psi_{\text{out}} = \frac{1}{\sqrt{2}} \left[R_{\hat{n}_1} R_{\hat{n}_2} e^{+\pi i \Phi / \Phi_0} + R_{\hat{n}_2} R_{\hat{n}_1} e^{-\pi i \Phi / \Phi_0} \right] \Psi_{\text{in}}, \quad (16)$$

where Φ is the magnetic flux encircled by the closed edge-channel loop, $\Phi_0 = h/e$ is the magnetic flux quantum, and $R_{\hat{n}_1, \hat{n}_2}$ are rotation operators in spin space which describe spin precession. The precession axis is parallel to the direction of the effective magnetic field, which de-

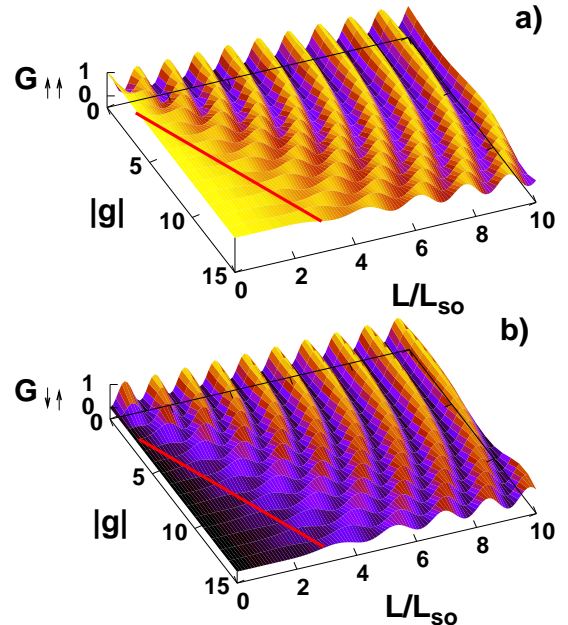


FIG. 5: (Color online) $G_{\uparrow\uparrow}$ (a) and $G_{\downarrow\uparrow}$ (b) plotted as a function of SO coupling strength and the g -factor g , at filling factor 1. The red line represents the points for which $|\nu_R/\nu_Z| = 1$. (We computed ν_R assuming $\nu_n^{(0)} = \omega_c l_B$, which is appropriate for a sharp edge potential.) The other parameters are: $E_F/\hbar\omega_c = 1$, $L/\lambda_F = 40$, $W/\lambda_F = 2$.

pends on the directions of the electron motion and the Zeeman field. In our simple setup, it can be directed along \hat{n}_1 and \hat{n}_2 , depending on the side of the interferometer on which the electron is traveling. (See Fig. 6.) Explicitly, the rotation operator reads

$$R_{\hat{n}_j} = e^{-i\frac{\pi L}{L_{\text{so}}}\vec{\sigma}\cdot\hat{n}_j}, \quad (17)$$

with $j = 1, 2$, and $\hat{\sigma}$ denoting the vector of Pauli matrices. Let us consider the case $\Phi/\Phi_0 = n$ (constructive interference due to the magnetic field). To obtain destructive interference in this situation, we need that

$$R_{\hat{n}_1}R_{\hat{n}_2} + R_{\hat{n}_2}R_{\hat{n}_1} = 0 \quad (18)$$

holds. If the sides of the interferometer are perpendicular and the Zeeman term is negligible, the two directions \hat{n}_1 and \hat{n}_2 are orthogonal and, hence, $\sigma_{\hat{n}_1}\sigma_{\hat{n}_2} + \sigma_{\hat{n}_2}\sigma_{\hat{n}_1} = 0$. If this is the case, the condition Eq. (18) for destructive interference becomes $L = (n + 1/2)L_{\text{so}}$. A similar result was found in Ref. 46 where the localization of electrons in quantum-coherent networks due to Rashba SO coupling was discussed. We conclude that by varying the Rashba coupling in our interferometer configuration realized with edge states, it is possible to obtain a current modulation at a fixed magnetic field. This setup would be a realization of the spin interferometer proposed in Ref. 44, which is based on spin precession due to the Rashba effect in a ring geometry.

V. CONCLUSIONS

We have obtained analytical results, valid in the high-magnetic-field regime, for quantum-Hall edge channels

in the presence of Rashba spin-orbit coupling and Zeeman splitting. Rashba spin precession is expected to occur due to the relative shift of spin-polarized Landau levels in guiding-center direction. Furthermore, we have presented results on the effect of spin precession on edge-channel transport obtained by a recursive Green's-function method. Finally, we have proposed the realization of a spin-dependent interferometer based on spin-precession of electrons in quantum-Hall edge channels.

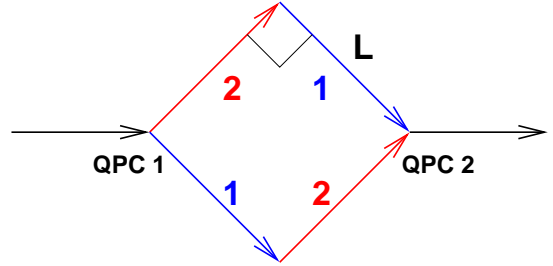


FIG. 6: (Color online) Schematic view of the simplest interferometer setup. A right-moving edge channel is split, via quantum point contact 1 (QPC1), and recombines at a second quantum point contact (QPC2).

Acknowledgments

The authors would like to thank D. Frustaglia for useful discussions and helpful suggestions. This work has been supported by the IST NANOTCAD project (EU contract IST-1999-10828), an EU Research Training Network (RTN2-2001-00440), and the MacDiarmid Institute of Advanced Materials and Nanotechnology (New Zealand).

¹ D. D. Awschalom, D. Loss, and N. Samarth (Eds.), *Semiconductor Spintronics and Quantum Computation*, Series Nanoscience and Technology (Springer, Berlin, 2002).

² I. Zutic, J. Fabian, and S. Das Sarma, Rev. Mod. Phys. **76**, 323 (2004).

³ S. A. Wolf, D. D. Awschalom, R. A. Buhrman, J. M. Daughton, S. von Molnár, M. L. Roukes, A. Y. Chtchelkina, and D. M. Treger, Science **294**, 1488 (2001).

⁴ G. A. Prinz, Science **282**, 1660 (1998).

⁵ S. Datta and B. Das, Appl. Phys. Lett. **56**, 665 (1990).

⁶ E. A. de Andrade e Silva and G. C. La Rocca, Phys. Rev. B **59**, R15583 (1999); A. A. Kiselev and K. W. Kim, Appl. Phys. Lett. **78**, 775, (2001); T. Koga, J. Nitta, H. Takayanagi, and S. Datta, Phys. Rev. Lett. **88**, 126601 (2001); M. Governale, D. Boese, U. Zülicke, and C. Schroll, Phys. Rev. B **65**, 140403(R) (2002); R. Ionicioiu and I. D'Amico, Phys. Rev. B **67**, 041307(R) (2003); J. C. Egues, G. Burkard, and D. Loss, Phys. Rev. Lett. **89**, 176401 (2002); M. Governale, Phys. Rev. Lett., **89**, 206802 (2002); L. S. Levitov and E. I. Rashba, Phys. Rev. B **67**, 115324 (2003); M. Governale, F. Taddei, and R. Fazio, Phys. Rev. B **68**, 155324 (2003); M. G. Pala, M. Governale, J. König, U. Zülicke, and G. Iannaccone, Phys. Rev. B **69**, 045304 (2004).

⁷ E. I. Rashba, Fiz. Tverd. Tela (Leningrad) **2**, 1224 (1960) [Sov. Phys. Solid State **2**, 1109 (1960)].

⁸ G. Lommer, F. Malcher, and U. Rössler, Phys. Rev. Lett. **60**, 728 (1988).

⁹ E. A. de Andrade e Silva, G. C. La Rocca, and F. Bassani, Phys. Rev. B **50**, 8523 (1994).

¹⁰ J. Nitta, T. Akazaki, H. Takayanagi, and T. Enoki, Phys. Rev. Lett. **78**, 1335 (1997).

¹¹ Th. Schäpers, G. Engels, J. Lange, Th. Klocke, M. Hollfelder, and H. Lth, J. Appl. Phys. **83**, 4324 (1998).

¹² D. Grundler, Phys. Rev. Lett. **84**, 6074 (2000).

¹³ Y. Sato, T. Kita, S. Gozu, and S. Yamada, J. Appl. Phys. **89**, 8017 (2001).

¹⁴ M. I. Dyakonov and V. I. Perel, Sov. Phys. JETP **33**, 1053 (1971); Sov. Phys. Solid State **13**, 3023 (1972).

¹⁵ R. E. Prange and S. M. Girvin (Eds.), *The Quantum Hall Effect*, 2nd ed. (Springer, New York, 1990).

¹⁶ B. I. Halperin, Phys. Rev. B **25**, 2185 (1984).

¹⁷ A. H. MacDonald and P. Středa, Phys. Rev. B **29**, 1616 (1984).

¹⁸ A not-so-strong confinement gives rise to the appearance of alternating compressible and incompressible strips of 2D electron fluid, and the description of transport gets more complex. See, e.g., D. B. Chklovskii, B. I. Shklovskii, and L. I. Glazman Phys. Rev. B **46**, 4026 (1992); D. B. Chklovskii, K. A. Matveev, and B. I. Shklovskii, *ibid.* **47**, 12605 (1993); K. Lier and R. R. Gerhardts, *ibid.* **50**, 7757 (1994); R. J. F. van Haren, F. A. P. Blom, and J. H. Wolter, Phys. Rev. Lett. **74**, 1198 (1995); Y. Y. Wei, J. Weis, K. v. Klitzing, and K. Eberl, *ibid.* **81**, 1674 (1998); A. Yacoby, H. F. Hess, T. A. Fulton, L. N. Pfeiffer and K. W. West, Sol. State Commun. **111**, 1 (1999). We do not consider this situation here.

¹⁹ G. Müller, D. Weiss, A. V. Khaetskii, K. von Klitzing, S. Koch, H. Nickel, W. Schlapp, and R. Lösch, Phys. Rev. B **45**, R3932 (1992).

²⁰ E. V. Deviatov, A. Würtz, A. Lorke, M. Yu. Melnikov, V. T. Dolgopolov, D. Reuter, and A. D. Wieck, Phys. Rev. B **69**, 115330 (2004).

²¹ A. V. Khaetskii, Phys. Rev. B **45**, R13777 (1992).

²² D. G. Polyakov, Phys. Rev. B **53**, 15777 (1996).

²³ M. I. D'yakonov and V. Yu. Kachorovskii, Fiz. Tekh. Poluprovodn. **20**, 178 (1986) [Sov. Phys. Semicond. **20**, 110 (1986)]; E. I. Rashba and E. Ya. Sherman, Phys. Lett. A **129**, 175 (1988).

²⁴ M. G. Pala, M. Governale, J. König, and U. Zülicke, Eur. phys. Lett. **65**, 850 (2004).

²⁵ S. A. Tarasenko and N. S. Averkiev, JETP Lett. **75**, 552 (2002).

²⁶ X. F. Wang and P. Vasilopoulos, Phys. Rev. B **67**, 085313 (2003).

²⁷ J. Wang, H. B. Sun, and D. Y. Xing, Phys. Rev. B **69**, 085304 (2004).

²⁸ G. Usaj and C. A. Balseiro, Phys. Rev. B **70**, 041301(R) (2004); A. Reynoso, G. Usaj, M. J. Sanchez, and C. A. Balseiro, cond-mat/0407138 (unpublished).

²⁹ L. P. Rokhinson, Yu. B. Lyanda-Geller, L. N. Pfeiffer, and K. W. West, cond-mat/0403645 (unpublished).

³⁰ F. Mireles and G. Kirczenow, Phys. Rev. B **64**, 024426 (2001).

³¹ M. Governale and U. Zülicke, Phys. Rev. B **66**, 073311 (2002); Sol. State Commun. **131**, 581 (2004).

³² G. Dresselhaus, Phys. Rev. **100**, 580 (1955).

³³ T. Koga, J. Nitta, T. Akazaki, and H. Takayanagi, Phys. Rev. Lett. **89**, 046801 (2002).

³⁴ S. D. Ganichev, V. V. Bel'kov, L. E. Golub, E. L. Ivchenko, P. Schneider, S. Giglberger, J. Eroms, J. De Boeck, G. Borghs, W. Wegscheider, D. Weiss, and W. Prettl, Phys. Rev. Lett. **92**, 256601 (2004).

³⁵ V. I. Fal'ko, Phys. Rev. Lett. **71**, 141 (1993).

³⁶ Th. Schäpers, J. Knobbe, and V. A. Guzenko, Phys. Rev. B **69**, 235323 (2004).

³⁷ R. Landauer, IBM J. Res. Dev. **1**, 233 (1957); M. Büttiker, Phys. Rev. Lett. **57**, 1761 (1986).

³⁸ H. U. Baranger, D. P. Di Vincenzo, R. A. Jalabert, and A. D. Stone, Phys. Rev. B **44**, 10637 (1991).

³⁹ D. K. Ferry and S. M. Goodnick, *Transport in Nanostructures* (Cambridge University Press, Cambridge, UK, 1997).

⁴⁰ D. Frustaglia, M. Hentschel, and K. Richter, Phys. Rev. Lett. **87**, 256602 (2001).

⁴¹ D. S. Fisher and P. A. Lee, Phys. Rev. B **23**, R6851 (1981).

⁴² F. E. Meijer, A. F. Morpurgo, T. M. Klapwijk, T. Koga, and J. Nitta, cond-mat/0406106 (unpublished).

⁴³ Y. Ji, Y. Chung, D. Sprinzak, M. Heiblum, D. Mahalu, and H. Shtrikman, Nature **422**, 415 (2003).

⁴⁴ J. Nitta, F. E. Meijer, and H. Takayanagi, Appl. Phys. Lett. **75**, 695 (1999).

⁴⁵ U. Zülicke, Appl. Phys. Lett. **85**, to appear (2004).

⁴⁶ D. Bercioux, M. Governale, V. Cataudella, and V. M. Ramaglia, Phys. Rev. Lett. **93**, 056802 (2004).